

# Effect of high-temperature treatment on Fe/ZSM-5 prepared by chemical vapor deposition of FeCl<sub>3</sub>

## II. Nitrous oxide decomposition, selective oxidation of benzene to phenol, and selective reduction of nitric oxide by isobutane

Q. Zhu, R.M. van Teeffelen, R.A. van Santen, and E.J.M. Hensen \*

*Schuit Institute of Catalysis, Laboratory of Inorganic Chemistry and Catalysis, Eindhoven University of Technology, PO Box 513, 5600 MB, Eindhoven, The Netherlands*

Received 30 June 2003; revised 19 September 2003; accepted 24 September 2003

### Abstract

The catalytic performance (nitrous oxide decomposition, hydroxylation of benzene to phenol with nitrous oxide, and selective reduction of nitric oxide by *i*-butane) was evaluated for a set of HZSM-5 and sublimed Fe/ZSM-5 catalysts, which have been extensively characterized in an earlier contribution (J. Catal. (2003)). Nitrous oxide decomposition rates for the sublimed samples strongly increase after high-temperature calcination and particularly, after high-temperature steaming. Only a small fraction of the total iron content is active in this decomposition. For benzene hydroxylation the initial phenol productivity also increases with increasing severity of treatment. It is concluded that similar catalytic sites are important. Nevertheless, Fe/ZSM-5 and Fe/ZSM-5(HTC) exhibit relatively low phenol selectivities due to significant hydrocarbon combustion. The steamed Fe/ZSM-5, however, produces phenol with high selectivity. The stability of the sublimed samples is relatively low due to the large coke make, attributable to the large number of active sites. Commercial HZSM-5 with an iron content of 0.024 wt% and its steamed counterpart are also active and have a better stability, the latter one having the highest phenol productivity after prolonged reaction times. The beneficial effect of severe activation treatments to sublimed Fe/ZSM-5, where iron is introduced at extraframework positions, is taken as an indication that removal of lattice aluminum is important for the generation of active sites. The different activity order in NO reduction by *i*-butane suggests that the active sites for this reaction are different from those for nitrous oxide decomposition and selective benzene oxidation.

© 2003 Elsevier Inc. All rights reserved.

**Keywords:** Fe/ZSM-5; Sublimation method; Active sites; Nitrous oxide decomposition; Benzene oxidation to phenol; NO SCR

### 1. Introduction

Iron-containing zeolitic materials with the MFI topology have been identified as potential catalysts for a large number of environmentally benign processes. Foremost, the reduction of nitrogen oxides by hydrocarbons or ammonia [1–8] has been a major topic in the field of environmental catalysis, because it may provide a technology for NO<sub>x</sub> abatement with diesel and lean-burn Otto engines. Promising performances in the decomposition of nitrous oxide have also been noted and are of potential value to the abatement of this notorious greenhouse gas in the tail gases of nitric acid plants

[5,9–15]. The high selectivity to phenol in the selective oxidation of benzene using nitrous oxide as oxidant is well known [16–19] and might form an alternative to the existing cumene process [20]. Other interesting reactions include the isomerization and dehydrogenation of alkanes [21] and the selective oxidation of ammonia [22].

The two most important preparation routes to active iron-containing MFI catalysts, i.e., isomorphous substitution of Fe in the MFI framework followed by activation or postsynthesis addition of Fe to ZSM-5 zeolite, have been discussed in some detail in a companion report [23]. In our view, it appears that Fe/ZSM-5 prepared by sublimation of FeCl<sub>3</sub> followed by washing and calcination, a widely applied technique [4,8,10,11,14,15,23–25], produces a material with a quite heterogeneous speciation of the iron. While the exact distribution of Fe species clearly depends on the pretreat-

\* Corresponding author.

E-mail address: [e.j.m.hensen@tue.nl](mailto:e.j.m.hensen@tue.nl) (E.J.M. Hensen).

ment procedure [23–31], we have addressed the changes upon severe high-temperature (973 K) treatments [23]. For sublimed Fe/ZSM-5, the largest fraction is present on the external surface as iron oxide/hydroxide crystallites, the remaining fraction being retained in the micropore space as neutral iron oxide nanoparticles and as charge-compensating complexes. Following interesting changes in the behavior of sublimed Fe/ZSM-5 in the decomposition of nitrous oxide by severe treatments, i.e., high-temperature (973 K) calcination or steaming [14,15], we have studied in detail the changes in the speciation of the various iron-containing phases [23]. A combination of  $^{57}\text{Fe}$  Mössbauer spectroscopy and low-temperature nitrous oxide decomposition points out that the amount of sites active in nitrous oxide activation is relatively low and increases with the number of  $\text{Fe}^{2+}$  centers. Severe treatment of Fe/ZSM-5 results in an increase of such centers. The sintering of the prevailing iron oxide phase is observed by TEM and by an increase of the ordering of such phases as derived from Fe  $K$ -edge EXAFS measurements. These trends are in line with the postulation that only a minor fraction of the iron species is active. Since the ability to activate nitrous oxide has been related to the selective conversion of benzene to phenol [19,32,33], we wanted to compare the catalytic activities of the present set of sublimed catalysts for this reaction. Commercial HZSM-5 with an iron content of 0.024 wt%, applied in calcined and steamed form, forms an analogue to the commonly applied iron-substituted ZSM-5 materials. Finally, in view of the intense debate on the active sites and the speculations that for NO reduction binuclear clusters are also important (e.g., [4]), we also determined the activity of the sublimed catalysts in the reduction of NO with *i*-butane.

## 2. Experimental

### 2.1. Materials

Details of the preparation and characterization of the catalytic materials are extensively described in a companion paper [23].

### 2.2. Activity testing

The catalytic reactions were carried out in a single-pass atmospheric microflow reactor system as schematically shown in Fig. 1. The catalyst was contained in a quartz reactor with an inner diameter of 4 mm. Gas flows (helium, oxygen, nitrous oxide, nitric oxide, *i*-butane) were regulated by well-calibrated thermal mass-flow controllers. Liquid benzene was fed to the reaction mixture by a Bronkhorst liquid mass-flow controller. To prevent condensation of phenol the stainless-steel lines were contained in an oven operated at 453 K and where needed heated by tracing. A combination of online gas chromatography (GC, HP-5, detection by FID) for analysis of benzene, phenol, *i*-butane, and other

hydrocarbon products and mass spectrometry (MS, Balzers TPG 215) for analysis of nitrous oxide, nitric oxide, oxygen, nitrogen and water was used. Calibration to determine the response factors of phenol was carried out by feeding a mixture of toluene, benzene, and phenol to the reactor system by a separate high-pressure liquid pump.

#### 2.2.1. Catalyst pretreatment

Prior to reaction, the catalyst was subjected to a calcination procedure. To this end, a sample was heated in an artificial air flow ( $100\text{ ml min}^{-1}$ , 20 vol%  $\text{O}_2$  in He) at a heating rate of  $1\text{ K min}^{-1}$  from room temperature to 823 K. After an isothermal period of at least 2 h, the reactor was cooled to the desired reaction temperature. For NO SCR experiments the catalyst was purged with He prior to reaction.

#### 2.2.2. Nitrous oxide decomposition

A concentration of 0.35 vol% (in some cases: 0.5 vol%) nitrous oxide in He at a GHSV of  $24,000\text{ h}^{-1}$  ( $30,000\text{ h}^{-1}$ ) was used for studying nitrous oxide decomposition.

#### 2.2.3. Benzene oxidation by nitrous oxide

The reaction mixture consisted of a mixture of 1 vol% benzene and 4 vol% nitrous oxide in helium. A total flow rate of  $100\text{ ml min}^{-1}$  was maintained at a total GHSV of  $30,000\text{ h}^{-1}$ . The carbon mass balance closed at 99%, while the nitrogen mass balance allowed accuracies up to 98%.

#### 2.2.4. Selective reduction of nitric oxide by isobutane

Reduction of NO by isobutane was carried out by feeding a mixture of 0.2 vol% NO, 0.2 vol% isobutane, 3 vol%  $\text{O}_2$  in He to the catalytic reactor. The total flow rate was  $200\text{ ml min}^{-1}$ , while a GHSV of  $42,000\text{ h}^{-1}$  was adopted. The temperature dependence of the reaction was tested in the following manner: a typical reaction was performed for 4 h while analyzing the reactor effluent continuously by MS and every 10 min by GC analysis. Subsequently, the catalyst was cooled to room temperature under a He flow. The catalyst was recalined by the earlier described procedure and tested at the next temperature. During the calcination of spent catalyst, carbon monoxide, carbon dioxide, and water were detected. Repetitive activity experiments at 673 K indicated that this calcination procedure leads to the regeneration of the initial state of the catalyst.

## 3. Results and discussion

### 3.1. Nitrous oxide decomposition

Table 1 summarizes the steady-state reaction rates for nitrous oxide decomposition of the various catalysts at a reaction temperature of 673 K. Generally, we observed that there is an initial period of high activity followed by a strong deactivation and a steady-state regime. Fig. 2 displays the gas-phase concentrations as a function of the time

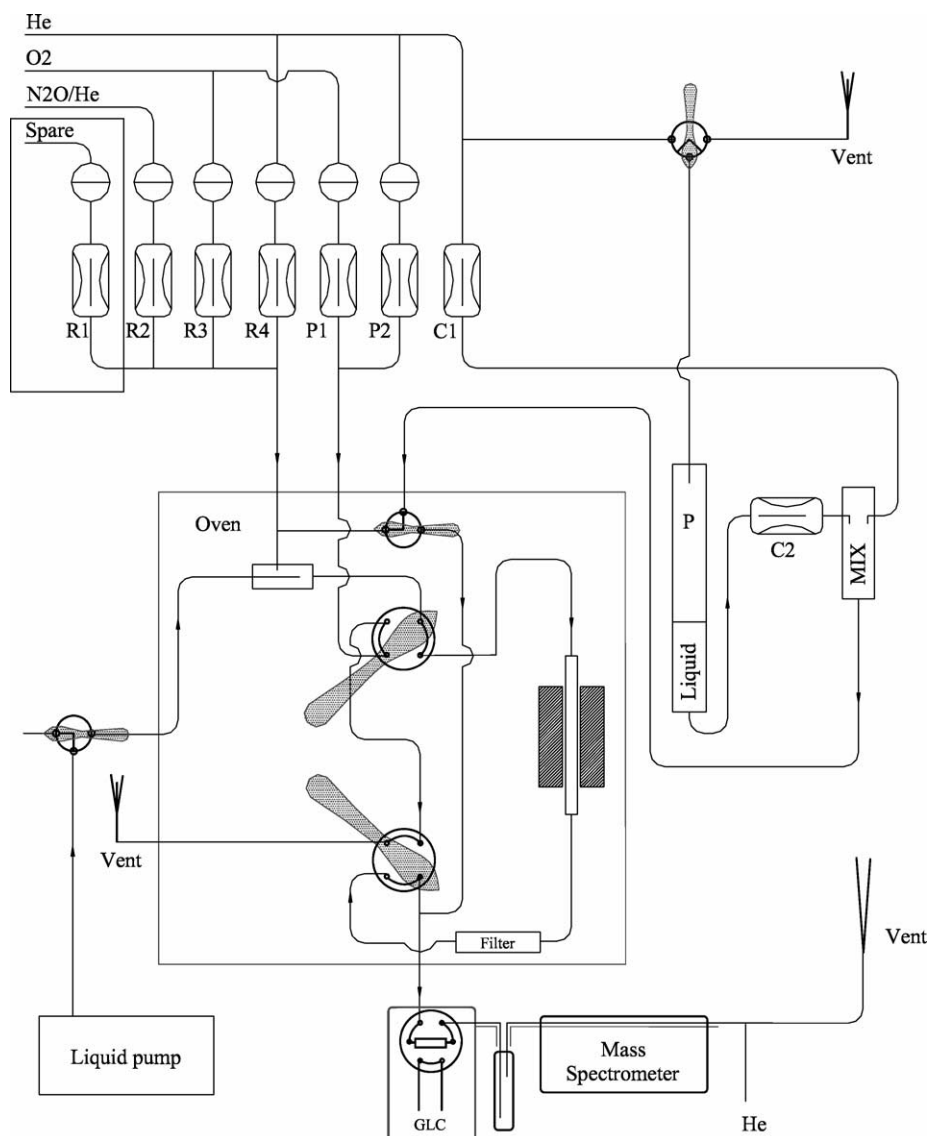


Fig. 1. Schematic layout of the reactor setup for nitrous oxide decomposition, benzene to phenol oxidation, and selective catalytic reduction of NO by isobutane.

Table 1

Steady-state reaction rates for the decomposition of nitrous oxide at a reaction temperature of 673 K ( $R$ ), the amount of oxygen atoms deposited after decomposition at 523 K ( $N_O$ ), and the amount of  $\text{Fe}^{2+}$  centers as determined from  $^{57}\text{Fe}$  Mössbauer measurements taken from Ref. [23]

Sample	$R$ ( $10^{-6} \text{ mol g}^{-1} \text{ s}^{-1}$ )	$N_O$ ( $\text{g}^{-1}$ )	$\text{Fe}^{2+}$ ( $\text{g}^{-1}$ )
Fe/ZSM-5	0.29	$0.58 \times 10^{19}$	$1.0 \times 10^{19}$
Fe/ZSM-5(HTC)	0.44	$1.5 \times 10^{19}$	$3.4 \times 10^{19}$
Fe/ZSM-5(HTS)	0.67	$1.9 \times 10^{19}$	$4.9 \times 10^{19}$

on stream for a typical nitrous oxide decomposition reaction over Fe/ZSM-5. Clearly, a strong decrease in conversion is observed after approximately 0.7 h. We suggest that the initial high activity is due to the presence of  $\text{Fe}^{2+}$  centers generated by autoreduction of iron oxide particles. Exposure to nitrous oxide results in a slow reoxidation of these sites and ultimately in their deactivation. Nevertheless, these

$\text{Fe}^{2+}$  species exhibit a relatively high nitrous oxide decomposition activity. The generation of these species by autoreduction is further supported by activity data of samples pretreated in different atmospheres. To this end, an amount of Fe/ZSM-5(HTS) was pretreated in various flows with a different oxygen concentration (total flow:  $100 \text{ ml min}^{-1}$  for 1 h at 658 K) before carrying out the nitrous oxide decomposition reaction. Fig. 3 displays the nitrous oxide conversion as a function of the time on stream for this set of experiments. Clearly, a He treatment results in a relatively long regime with high activity before a strong deactivation is observed and a steady state is attained. Subsequent treatment of the catalyst in 20 vol%  $\text{O}_2/\text{He}$  for 1 h at 658 K followed by exposure to the reaction mixture results in similar behavior. However, a much shorter deactivation period is observed. A similar treatment in pure  $\text{O}_2$  further reduces the deactivation period. Notably, the steady-state conversion is similar in all cases and a pretreatment in He at 658 K restores the

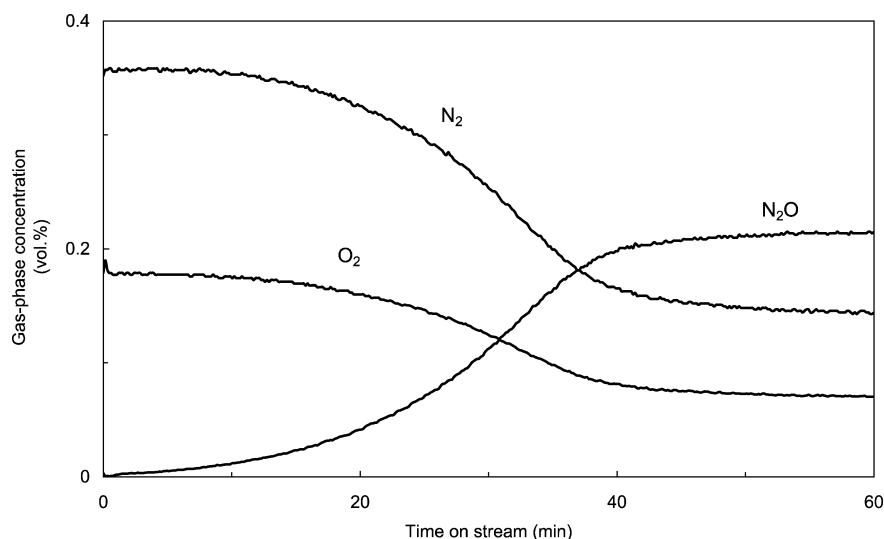


Fig. 2. Concentration of nitrous oxide, nitrogen, and oxygen during  $\text{N}_2\text{O}$  decomposition over Fe/ZSM-5. The reaction temperature is 698 K, while the feed nitrous oxide concentration is 0.35 vol% at a GHSV of  $24,000 \text{ h}^{-1}$ .

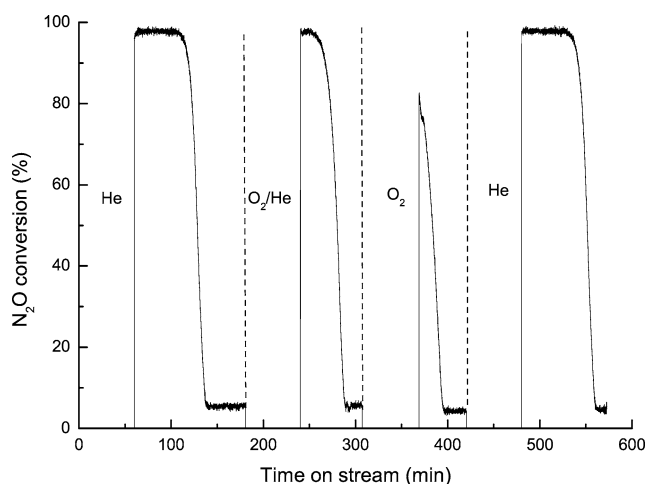


Fig. 3. Nitrous oxide conversion as a function of the time on stream for Fe/ZSM-5(HTS) with various intermittent regeneration procedures. Regeneration is carried out at a reaction temperature of 658 K by exposure to a flow ( $100 \text{ ml min}^{-1}$ ) of the indicated gas. The feed nitrous oxide concentration is 0.5 vol% at a GHSV of  $30,000 \text{ h}^{-1}$ .

initial long deactivation period. This deactivation is related to Fe species that can be oxidized by molecular oxygen as derived from the dependence on the oxygen partial pressure during pretreatment. The group of Panov [33–35] has shown that  $\text{Fe}^{2+}$  centers created upon high-temperature activation in FeZSM-5 and active in the catalytic nitrous oxide decomposition and related alkane oxidation cannot be reoxidized by molecular oxygen, possibly due to structural relaxation after the initial loss of molecular oxygen [33]. We thus believe that the high initial activity is caused by  $\text{Fe}^{2+}$  centers resulting from autoreduction of iron oxide particles at relatively high temperatures which are slowly reoxidized to  $\text{Fe}^{3+}$ . These particles include predominantly small nanometric iron oxide species in the micropores but also iron oxide aggregates on the external surface may play a role.

The observation that these centers can be reoxidized by oxygen (Fig. 3) agrees with their multinuclear nature, since it is reasonable to assume that activation of molecular oxygen requires a multinuclear site. The difference between these sites and the ones observed by  $^{57}\text{Fe}$  Mössbauer spectroscopy is that the latter species are able to decompose nitrous oxide at relatively low temperature [23]. Table 1 also lists the earlier reported values for the amount of deposited oxygen atoms by low-temperature nitrous oxide decomposition and the  $\text{Fe}^{2+}$  contribution derived from  $^{57}\text{Fe}$  Mössbauer spectroscopy under high-vacuum conditions at room temperature [23]. Clearly, the steady-state activity correlates to the number of sites active in the nitrous oxide decomposition. At least three species appear to be relevant: (i)  $\text{Fe}^{2+}$  species generated by autoreduction of aggregated iron oxide species which are reoxidized by nitrous oxide and do not further participate in the catalytic cycle, (ii) cationic iron oxide species compensating the framework charge with moderate activity, and (iii) a very small fraction of iron with the specific ability to decompose nitrous oxide at relatively low temperatures.

### 3.2. Benzene oxidation by nitrous oxide

The phenol productivities as a function of the time on stream for the various catalysts are shown in Fig. 4. Table 2 lists a number of reaction parameters after reaction times of 5 min, 1 h, and 5 h. Fe/SiO<sub>2</sub> did not show any activity for this reaction. In all other cases, we observe a high initial activity followed by a strong deactivation. Clearly, the initial activity is highest for Fe/ZSM-5(HTS) and the phenol productivity decreases in the order Fe/ZSM-5(HTS) > Fe/ZSM-5(HTC) > Fe/ZSM-5 for the sublimed catalysts. After prolonged reaction times, the conversion of the steamed sample is lowest, but the higher conversion of Fe/ZSM-5 and Fe/ZSM-5(HTC) is mainly due to combustion. Whereas the deactivation is relatively strong for

Table 2

Benzene conversion ( $X_{C_6H_6}$ ), benzene selectivity to phenol ( $S_{C_6H_6}$ ), nitrous oxide conversion ( $X_{N_2O}$ ) and nitrous oxide selectivity to phenol ( $S_{N_2O}$ ) for the various catalysts during benzene oxidation after reaction times ( $t_R$ ) of 5 min, 1 h, and 5 h

Sample	$R_{Ph,i}$	$t_R = 5 \text{ min}$				$t_R = 1 \text{ h}$				$t_R = 5 \text{ h}$			
		$X_{C_6H_6}$	$S_{C_6H_6}$	$X_{N_2O}$	$S_{N_2O}$	$X_{C_6H_6}$	$S_{C_6H_6}$	$X_{N_2O}$	$S_{N_2O}$	$X_{C_6H_6}$	$S_{C_6H_6}$	$X_{N_2O}$	$S_{N_2O}$
Fe/ZSM-5	3.7	23	47	35	7.8	11	18	32	1.5	10	6	35	0.4
Fe/ZSM-5(HTC)	6.5	32	60	36	13	14	27	40	2.3	13	9	51	0.5
Fe/ZSM-5(HTS)	8.5	39	82	21	38	12	> 99	5	66	3	> 99	4	26
HZSM-5	2.6	18	60	4	60	7	> 99	2	> 98	4	> 99	1	> 98
HZSM-5(HTS)	5.4	31	61	5	94	13	> 99	3	> 98	9	> 99	2.3	> 98
Fe/SiO <sub>2</sub>	0	0	0	0	0	0	0	0	0	0	0	0	0

Additionally, the initial phenol productivity—extrapolated to zero reaction time—is given ( $R_{Ph,i}$  in  $\text{mmol g}^{-1} \text{h}^{-1}$ ).

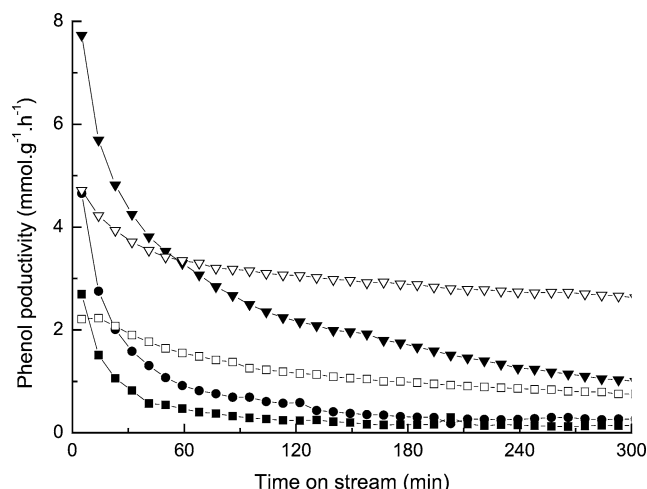


Fig. 4. Phenol productivities during benzene hydroxylation (total flow  $100 \text{ ml min}^{-1}$ ; feed, 1 vol%  $C_6H_6$ , 4 vol%  $N_2O$  in He;  $T = 623 \text{ K}$ ) for (■) Fe/ZSM-5, (●) Fe/ZSM-5(HTC), (▼) Fe/ZSM-5(HTS), (□) HZSM-5, and (▽) HZSM-5(HTS).

these catalysts, HZSM-5(HTS) shows a lower initial activity than Fe/ZSM-5(HTS), but a pronouncedly higher stability. In fact, this catalyst has the highest phenol productivity after prolonged reaction times. Large differences in selectivities to phenol are observed between the various catalysts. HZSM-5 and HZSM-5(HTS) exhibit initial benzene selectivities around 50–60% which increase to over 99% within 1 h. On the other hand, the nitrous oxide selectivity is over 90% already at relatively low reaction times, implying that the initial lower benzene selectivity is due to the buildup of some coke products on the catalyst surface. The absence of carbon monoxide, carbon dioxide, and water confirms that the lower selectivity is not due to combustion. Results from nitrogen adsorption experiments and gravimetric analyses of fresh and spent samples are collected in Table 3. Clearly, the decrease in micropore volume and surface area is relatively small for HZSM-5 and HZSM-5(HTS) and the coke content after a reaction time of 5 h is considerably smaller than for the sublimed catalysts. These observations are in line with the lower deactivation rate of the HZSM-5 catalysts. HZSM-5 and HZSM-5(HTS) show similar catalytic behavior. We attribute the catalytic activity of these catalysts to the presence of extraframework Fe species rather than to Brøn-

Table 3

Micropore volumes ( $V_{Lang}$ ) and nitrogen surface areas ( $S_{Lang}$ ) determined by the Langmuir equation of the various catalysts before and after benzene oxidation and the amount of coke formed during benzene oxidation

Sample	Before benzene oxidation		After benzene oxidation		Coke (wt%)
	$V_{Lang}$ ( $\text{ml g}^{-1}$ )	$S_{Lang}$ ( $\text{m}^2 \text{g}^{-1}$ )	$V_{Lang}$ ( $\text{ml g}^{-1}$ )	$S_{Lang}$ ( $\text{m}^2 \text{g}^{-1}$ )	
Fe/ZSM-5	0.119	334	0.013	36	10.3
Fe/ZSM-5(HTC)	0.121	341	0.020	56	11.0
Fe/ZSM-5(HTS)	0.132	371	0.084	237	3.2
HZSM-5	0.156	440	0.150	420	n.d. <sup>a</sup>
HZSM-5(HTS)	0.161	456	0.143	404	2.1

<sup>a</sup> Not determined.

sted acid sites [36,37] or Lewis Al sites [38–40]. Brønsted acid sites do not appear to play a prominent role since removal of the Brønsted acidity of HZSM-5 by steaming [23] increases the activity. Moreover, the presence of these strong Brønsted acid sites does not impart a much larger coking deactivation compared to the case where such sites are absent. This appears to contrast the recent conclusion by Meloni et al. [41]. Recent work from our group [42] provides evidence that Fe is a required component for active oxidation catalysts because a hydrothermally synthesized HZSM-5 sample with a very low iron content exhibited a negligible activity at 623 K in line with earlier propositions [19,41,43,44]. The activity of the nonsteamed HZSM-5 appears to be related to some kind of extraframework iron species, already present after template removal [23].

The initial benzene conversion for Fe/ZSM-5(HTS) is around 40% with a benzene selectivity around 80%. In contrast to HZSM-5(HTS), the nitrous oxide selectivity is relatively low and considerable amounts of CO, CO<sub>2</sub>, and H<sub>2</sub>O are detected. With increasing reaction times, phenol is produced with high selectivity, although the phenol productivity is quite low ( $\sim 1.0 \text{ mmol g}^{-1} \text{h}^{-1}$ ) due to the strong deactivation. Despite the high selectivity of benzene to phenol at higher reaction times, the nitrous oxide selectivity remains far below 100%. Thus, part of the nitrous oxide is used for combustion of coke residue that was initially deposited. This is corroborated by an increase of the effluent CO<sub>2</sub> concentration with reaction time. Conversely, Fe/ZSM-5 and Fe/ZSM-5(HTC) produce much higher amounts of combustion products, leading to poor benzene and nitrous oxide

selectivities. Although not totally clear, the presence of iron oxide nanoparticles in the micropores may be the reason for the larger amount of hydrocarbon combustion for these two catalysts. Alternatively, one may also suggest that cationic Fe species contribute to the combustion of benzene. Their number should be smaller in the catalyst with a low iron content (HZSM-5) and in the steamed Fe/ZSM-5 catalyst. This may be due to oxidation by molecular oxygen formed by nitrous oxide decomposition on such cationic species or directly by deposited oxygen atoms from nitrous oxide. The corresponding data in Table 3 confirm that the coking deactivation for Fe/ZSM-5 and Fe/ZSM-5(HTC) is more pronounced than for Fe/ZSM-5(HTS) and the HZSM-5 samples. The micropore volume and surface area are strongly reduced after 5 h of reaction. Clearly, the decrease in these accessibility parameters for Fe/ZSM-5(HTS) is intermediate to those in Fe/ZSM-5(HTC) and HZSM-5(HTS). We surmise that the presence of small iron oxide nanoparticles in the micropores of Fe/ZSM-5 and Fe/ZSM-5(HTC) is detrimental for the stability of these catalysts, although it is not clear what the mechanism of coke formation is in this case. It might be that the resulting lower micropore volume of Fe/ZSM-5 and Fe/ZSM-5(HTC) [23] hinders the diffusion of larger product molecules such as traces of dihydroxybenzenes leading to pore blocking. HZSM-5, HZSM-5(HTS), and Fe/ZSM-5(HTS) show a much higher stability. Among them, Fe/ZSM-5(HTS) exhibits the strongest deactivation to be attributed to the larger number of active sites. As outlined by Meloni et al. [41], the coke deposits in benzene oxidation are made up by overoxidized phenol and condensed polyphenols. This implies that overoxidation of phenol is important in the formation of coke, providing an explanation for the stronger deactivation rate for those catalysts with a high initial activity.

The highest initial activity of Fe/ZSM-5(HTS) is in line with the highest number of sites active in the low-temperature nitrous oxide decomposition. For the sublimed samples, the activity decreases in the order Fe/ZSM-5(HTS) > Fe/ZSM-5(HTC) > Fe/ZSM-5. This coheres with the notion of formation of phenol upon interaction of benzene with an oxygen atom deposited from nitrous oxide [19]. Although the number of active sites for nitrous oxide decomposition for HZSM-5(HTS) is at least one order of magnitude smaller than for the sublimed samples, the differences in benzene oxidation are much less pronounced. It might very well be that the decreased pore volume of Fe/ZSM-5(HTS) impedes stronger diffusion limitations to benzene and phenol compared to HZSM-5(HTS). An alternative explanation might be that the initial activity of Fe/ZSM-5(HTS) is much higher than the value obtained by linear extrapolation (Table 2). This is indeed suggested from the more pronounced deactivation of Fe/ZSM-5(HTS) in Fig. 4. In that case, initial coke make in the first stages of the reaction will result in the deactivation of a large amount of active sites either by pore blocking or coke covering active sites. Based on a comparison of the titrated sites in HZSM-

5(HTS) and Fe/ZSM-5(HTS) a theoretical initial productivity of  $150 \text{ mmol g}^{-1} \text{ h}^{-1}$  for the latter sample is calculated. Thus, possibly Fe/ZSM-5(HTS) has a very high initial activity followed by a strong decrease in the first minutes of the reaction.

Our study confirms that sublimation of  $\text{FeCl}_3$  onto HZSM-5 zeolite is not the preferred preparation method for effective catalysts for benzene oxidation to phenol. Steaming, however, strongly increases the selectivity to phenol of sublimed Fe/ZSM-5. This hydrothermal treatment results in an increase of the number of active sites for low-temperature nitrous oxide decomposition [23], which is much higher than the number of active sites in HZSM-5(HTS). The rate of phenol formation is also strongly increased. The hydrothermal treatment also induces the migration of a fraction of neutral iron oxide particles from the micropores to the external surface which results in a more accessible catalyst pore structure. The creation of mesopores may also be important.

Brønsted acidity does not appear to be very important since HZSM-5 and HZSM-5(HTS) show similar reaction patterns. The higher activity of the latter one is generally explained by the higher number of iron active sites created due to more extensive Fe extraction from the lattice [44]. However, the very fact that high-temperature steaming is also beneficial for sublimed catalysts, in which the majority of Fe species was introduced at extraframework positions, points to a possible role of extraframework Al species. Regarding the role of Lewis Al sites, we note that the parent HZSM-5 material already contains some amount of extraframework Al species as followed from  $^{27}\text{Al}$  NMR measurements [23]. A speculative mechanism for the formation of the active sites in sublimed catalysts consists of two steps. First, the reaction of neutral iron oxide nanoparticles with Brønsted protons (protolysis) increases the number of cationic Fe species [15,23]. This occurs at elevated temperatures and is more extensive at higher temperatures (Fe/ZSM-5(HTC) versus Fe/ZSM-5). These cationic species are active in nitrous oxide decomposition and contribute to the combustion of benzene. Some dealumination probably takes place at elevated temperatures, leading to the formation of a higher number of active sites for selective benzene oxidation. Recently, strong indications have been provided by Hensen et al. [42] for the relevance of extraframework mixed Fe–Al oxo (Fe–Al–O) species to the selective benzene conversion with nitrous oxide. The presence of water during the high-temperature treatment (Fe/ZSM-5(HTS)) facilitates the extraction of Al. This will lead to the creation of more mixed Fe–Al–O species and a decrease of the amount of cationic species. This interpretation also has validity for catalyst precursors where Fe is isomorphously substituted in the framework. A study by Pérez-Ramírez et al. [45] showed that a significant part of the Fe is extracted from the lattice already during template removal, which agrees with our UV-Vis data on HZSM-5 indicating some amount of extraframework Fe species in the calcined precursor [23]. Nevertheless, most reports on the application of isomorphously

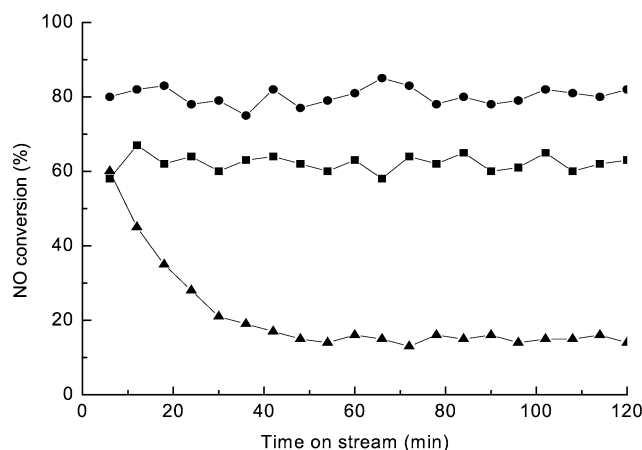


Fig. 5. NO conversion as a function of the time on stream (total flow  $100 \text{ ml min}^{-1}$ ; feed, 0.2 vol% NO, 0.2 vol%  $i\text{-C}_4\text{H}_8$ , 3 vol%  $\text{O}_2$  in He;  $T = 623 \text{ K}$ ) for (■) Fe/ZSM-5, (●) Fe/ZSM-5(HTC), and (▲) Fe/ZSM-5(HTS).

substituted ZSM-5 catalysts for benzene oxidation stress the importance of steaming [17,19,43] or alternatively high-temperature calcination [33] for such samples. The necessity of such treatments might thus be related to the creation of extraframework Al sites rather than to the extraction of additional Fe from the lattice. This notion agrees with the higher stability of Si–O–Al bonds compared to Si–O–Fe bonds. The relevance of Al extraction for active catalysts has been stressed in the study of Motz et al. [40], although these authors attributed the activity solely to extraframework Al sites and did not take into account the importance of the minute amounts of iron. Another indication supporting this proposal is provided in the study of Dubkov et al. [33] who found that impregnation of a small amount of  $\text{FeCl}_3$  in HZSM-5 followed by severe activation resulted in active sites similar to those in samples obtained via isomorphous substitution of iron in ZSM-5.

### 3.3. SCR of NO by isobutane

The conversion of NO as a function of the time on stream for the various catalysts is plotted in Fig. 5. Stable NO conversions are obtained for Fe/ZSM-5 and Fe/ZSM-5(HTC). Surprisingly, the steamed material shows a strong deactivation with increasing reaction times. Whereas the initial conversion is close to that of Fe/ZSM-5, a stable lower activity is obtained after prolonged reaction times. The temperature dependence of the conversion of NO and  $i$ -butane into  $\text{N}_2$ ,  $\text{H}_2\text{O}$ , CO, and  $\text{CO}_2$  for the various catalysts is plotted in Fig. 6. The light-off temperature of the NO reduction is around 523 K. A maximum in NO conversion is observed for the three sublimed catalysts. This is largely in accordance with the results reported by Chen and Sachtleir [25], although we find a somewhat lower maximum NO conversion for Fe/ZSM-5. For the present set of catalysts, the maximum in activity is found for Fe/ZSM-5(HTC) at a temperature of 623 K. The steamed sample has its maximum in

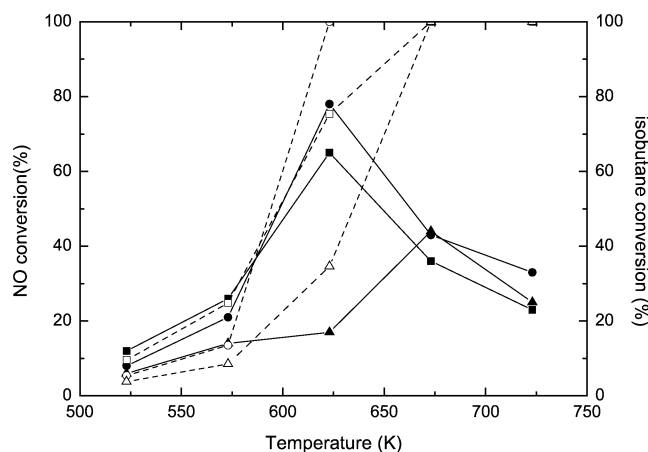


Fig. 6. NO and  $i$ -butane conversion as a function of the reaction temperature for (■,□) Fe/ZSM-5, (●,○) Fe/ZSM-5(HTC), and (▲,△) Fe/ZSM-5(HTS). Closed symbols refer to NO conversion, open symbols to  $i$ -butane conversion.

activity around 673 K where it is the most active catalyst. Whereas the high-temperature calcined sample has a considerably higher activity in the temperature window between 600 and 700 K, the relative order in activity below 600 K is Fe/ZSM-5 > Fe/ZSM-5(HTC) > Fe/ZSM-5(HTS). A comparison at relatively low temperatures is most relevant, since at elevated temperatures oxidation of the hydrocarbon by oxygen is dominant [25] as indicated by the decreased NO conversion. This activity order for the selective reduction of NO by  $i$ -butane is totally different from the order of the nitrous oxide decomposition and benzene-to-phenol transformation. This strongly suggests that the active sites for nitrous oxide activation are different from those for NO reduction. This is not too surprising in view of the proposed mechanism for the latter reaction. The first step consists of the conversion of NO to  $\text{NO}_2$  by  $\text{O}_2$ , followed by the reaction of nitrogen dioxide with carbonaceous deposits when a hydrocarbon is the reductant [46] and with  $\text{NH}_4^+$  when ammonia is [7]. Although it has been promoted [25,47] that this step takes place over cationic iron complexes, we expect that  $\text{NO}_2$  formation is not a very structure-sensitive reaction and proceeds over various types of iron species. This appears to agree with the fact that the NO SCR reaction is catalyzed by a wide range of oxides [48]. The activity order for the present set of catalysts points to the importance of the iron oxide phase dispersion for a high activity in NO reduction. The growth of these occluded iron oxide particles and migration from the micropores upon severe treatment [23] reduce the number of active sites for  $\text{NO}_2$  formation. We surmise that the low activity in the steamed catalyst is due to an imbalance between the formation of carbonaceous deposits and the generation of  $\text{NO}_2$  to remove them. This explains the relatively high initial activity which decreases strongly when deposits fill up the pores and block the active sites. This is most probably also related to the lower content of Brønsted acid sites which can redisperse iron oxide particles. This phenomenon has been described in detail by the

group of Sachtler [47,49] who showed that NaOH treatment negatively affected the NO oxidation activity by inducing the growth of iron oxide particles. The preference for the steamed sample at elevated temperatures, combustion of the hydrocarbon by molecular oxygen being dominant, could be due to the more open-pore architecture of this sample. Summarizing, we can conclude that the active sites for nitrous oxide decomposition are different from those for the selective reduction of nitric oxide with hydrocarbons. The latter reaction is catalyzed by a variety of small iron oxide particles in line with earlier observations [8].

#### 4. Conclusions

A set of sublimed Fe/ZSM-5 catalysts was tested in nitrous oxide decomposition, the conversion of benzene to phenol with nitrous oxide and hydrocarbon selective reduction of NO. The nitrous oxide decomposition rate for the sublimed samples strongly increases after high-temperature calcination and most notably after high-temperature steaming. The activities correlate to the earlier reported low-temperature nitrous oxide titration and point to the relevance of a minor fraction of the total iron content in the catalysis. This is valid for the steady-state activities. The initial strong deactivation is due to reoxidation of Fe<sup>2+</sup> centers generated by autoreduction of iron oxide particles at elevated temperatures. The activities in the hydroxylation of benzene of these samples increase with increasing severity of treatment. Nevertheless, Fe/ZSM-5 and Fe/ZSM-5(HTC) exhibit relatively low phenol selectivities due to significant hydrocarbon combustion. Only the steamed Fe/ZSM-5 produces phenol with high selectivity. The stability of the sublimed samples is relatively low due to the relatively large coke make. Commercial HZSM-5 with an iron content of 0.024 wt% and its steamed counterpart are also active and provide a higher stability, the latter one exhibiting the highest stable activity. We propose that extraframework Al sites are involved in the formation of active sites in addition to extraframework Fe sites, providing an explanation for the necessity of the widely reported severe activation treatments. NO reduction by *i*-butane does not require those sites with the property to activate nitrous oxide at low temperatures and dispersed iron oxide nanoparticles appear to be more important. This explains the decrease in NO reduction activity with increasing severity of treatment.

#### References

- [1] X. Feng, W.K. Hall, Catal. Lett. 41 (1996) 45.
- [2] X. Feng, W.K. Hall, J. Catal. 166 (1997) 368.
- [3] L.J. Lobree, I.-C. Hwang, J.A. Reimer, A.T. Bell, Catal. Lett. 63 (1999) 233.
- [4] H.-Y. Chen, T. Voskoboinikov, W.M.H. Sachtler, Catal. Today 54 (1999) 483.
- [5] G. Centi, F. Vazzana, Catal. Today 53 (1999) 683.
- [6] R.Q. Long, R.T. Yang, J. Am. Chem. Soc. 121 (1999) 5595.
- [7] R.Q. Long, R.T. Yang, J. Catal. 207 (2002) 224.
- [8] F. Heinrich, C. Schmidt, E. Löffler, M. Menzel, W. Grünert, J. Catal. 212 (2002) 157.
- [9] M. Rauscher, K. Kesore, R. Mönning, W. Schwieger, A. Tissler, T. Turek, Appl. Catal. A 184 (1999) 249.
- [10] El.-M. El Malki, R.A. van Santen, W.M.H. Sachtler, Micropor. Mesopor. Mater. 35–36 (2000) 235.
- [11] El.-M. El-Malki, R.A. van Santen, W.M.H. Sachtler, J. Catal. 196 (2000) 212.
- [12] J. Pérez-Ramírez, F. Kapteijn, G. Mul, X. Xu, J.A. Moulijn, Catal. Today 76 (2002) 55.
- [13] J. Pérez-Ramírez, F. Kapteijn, G. Mul, J.A. Moulijn, Chem. Commun. (2001) 693.
- [14] Q. Zhu, B.L. Mojet, R.A.J. Janssen, E.J.M. Hensen, J. Van Grondelle, P.C.M.M. Magusin, R.A. van Santen, Catal. Lett. 81 (2002) 205.
- [15] Q. Zhu, E.J.M. Hensen, B.L. Mojet, J.H.M.C. van Wolput, R.A. van Santen, Chem. Commun. (2002) 1232.
- [16] V.I. Sobolev, K.A. Dubkov, E.A. Paukshtis, L.V. Pirutko, M.A. Rodkin, A.S. Kharitonov, G.I. Panov, Appl. Catal. A 141 (1996) 185.
- [17] A. Ribera, I.W.C.E. Arends, S. de Vries, J. Pérez-Ramírez, R.A. Sheldon, J. Catal. 195 (2000) 287.
- [18] P. Kubánek, B. Wichterlová, Z. Sobalík, J. Catal. 211 (2002) 109.
- [19] G.I. Panov, CatTech 4 (2000) 18.
- [20] A.K. Uriarte, M.A. Rodkin, M.J. Gross, A.S. Kharitonov, G.I. Panov, Stud. Surf. Sci. Catal. 110 (1997) 857.
- [21] P.B. Venuto, Micropor. Mater. 2 (1994) 297.
- [22] R.Q. Long, R.T. Yang, Chem. Commun. (2000) 1651.
- [23] E.J.M. Hensen, Q. Zhu, M.M.R.M. Hendrix, A.R. Overweg, P.J. Kooyman, M.V. Sychev, R.A. van Santen, J. Catal., in press.
- [24] A. Dubkov, N.S. Ovanesyan, A.A. Shteinman, K.A. Dubkov, V.I. Sobolev, G.I. Panov, Kinet. Catal. 39 (1998) 792.
- [25] H.-Y. Chen, W.M.H. Sachtler, Catal. Today 42 (1998) 73.
- [26] R. Joyner, M. Stockenhuber, J. Phys. Chem. B 103 (1999) 5963.
- [27] M. Kögel, R. Mönning, W. Schwieger, A. Tissler, T. Turek, J. Catal. 182 (1999) 470.
- [28] P. Marturano, A. Kogelbauer, R. Prins, J. Catal. 190 (2000) 460.
- [29] P. Marturano, L. Drozdová, A. Kogelbauer, R. Prins, J. Catal. 192 (2000) 236.
- [30] A.A. Battiston, J.H. Bitter, D.C. Koningsberger, Catal. Lett. 66 (2000) 75.
- [31] A.A. Battiston, J.H. Bitter, F.M.F. de Groot, A.R. Overweg, O. Stephan, J.A. van Bokhoven, P.J. Kooyman, C. van der Spek, G. Vankó, D.C. Koningsberger, J. Catal. 213 (2003) 251.
- [32] G.I. Panov, G.A. Sheveleva, A.S. Kharitonov, V.N. Romannikov, L.A. Vostrikova, Appl. Catal. A 82 (1992) 31.
- [33] K.A. Dubkov, N.S. Ovanesyan, A.A. Shteinman, E.V. Starokon, G.I. Panov, J. Catal. 207 (2002) 341.
- [34] K.A. Dubkov, V.I. Sobolev, E.P. Talsi, M.A. Rodkin, N.H. Watkins, A.A. Shteinman, G.I. Panov, J. Mol. Catal. 123 (1997) 155.
- [35] G.I. Panov, V.I. Sobolev, K.A. Dubkov, V.N. Parmon, N.S. Ovanesyan, A.E. Shilov, A.A. Shteinman, React. Kinet. Catal. Lett. 61 (1997) 251.
- [36] E. Suzuki, K. Nakashiro, Y. Ono, Chem. Lett. (1988) 953.
- [37] R. Burch, C. Howitt, Appl. Catal. A 103 (1993) 135.
- [38] V.L. Zholobenko, I.N. Senchenya, L.M. Kustov, V.B. Kazansky, Kinet. Catal. 32 (1991) 151.
- [39] L.M. Kustov, A.L. Tarasov, V.I. Bogdan, A.A. Tyrlov, J.W. Fulmer, Catal. Today 61 (2000) 123.
- [40] J.L. Motz, H. Heinrich, W.F. Hölderich, J. Mol. Catal. 136 (1998) 175.
- [41] D. Meloni, R. Monaci, V. Solinas, G. Berlier, S. Bordiga, I. Rossetti, C. Oliva, L. Forni, J. Catal. 214 (2003) 169.
- [42] E.J.M. Hensen, Q. Zhu and R.A. van Santen, J. Catal., in press.
- [43] P. Kubánek, B. Wichterlová, Z. Sobalík, J. Catal. 211 (2002) 109.
- [44] G. Berlier, A. Zecchina, G. Spoto, G. Ricchiardi, S. Bordiga, C. Lamberti, J. Catal. 215 (2003) 264.



- [45] J. Pérez-Ramírez, G. Mul, F. Kapteijn, J.A. Moulijn, A.R. Overweg, A. Doménech, A. Ribera, I.W.C.E. Arends, *J. Catal.* 207 (2002) 113.
- [46] H.-Y. Chen, T. Voskoboinikov, W.M.H. Sachtler, *J. Catal.* 180 (1998) 171.
- [47] H.-Y. Chen, X. Wang, W.M.H. Sachtler, *PCCP* 2 (2000) 3083.
- [48] H. Bosch, F. Janssen, *Catal. Today* 2 (1988) 369.
- [49] H.-Y. Chen, E.-M. El-Malki, X. Wang, R.A. van Santen, W.M.H. Sachtler, *J. Mol. Catal. A* 162 (2000) 159.